

# **CHAPTER 2**

## **DESCRIPTION OF THE EXPERIMENTAL APPARATUS AND DIAGNOSTICS SET-UP**

### **2.1 The MPD thruster**

#### **2.1.1 Introduction**

Magneto-plasma-dynamic thrusters (MPD) are electromagnetic accelerators proposed for spacecraft propulsion. The gas is accelerated through the action of the Lorentz force reaching exhaust velocities in the range of 10-80 km/s [20]. Due to their power and the duration of their operation, MPD thrusters are suitable for long missions as the interplanetary ones [22]. At high power, critical regimes of the MPD thruster are observed. This limits its performance. Experimental investigations show that, beyond a critical value, oscillations in the discharge current seem to occur. At the same time, the anode losses increase and lead to a strong decrease of the efficiency.

This section describes the optical set-up of an investigation of an hybrid plasma MPD thruster. The investigation is carried out in the framework of the project *Experimental Investigation on a Magneto-Plasma-Dynamics Thrusters for Space Applications*, sponsored by the Italian Ministry of the University and the Scientific Research (MURST-MIUR).

### 2.1.2 Description of the experimental apparatus

A schematic description of the experimental apparatus developed in the laboratories of Centrosazio in Pisa is given in figure 2.1.

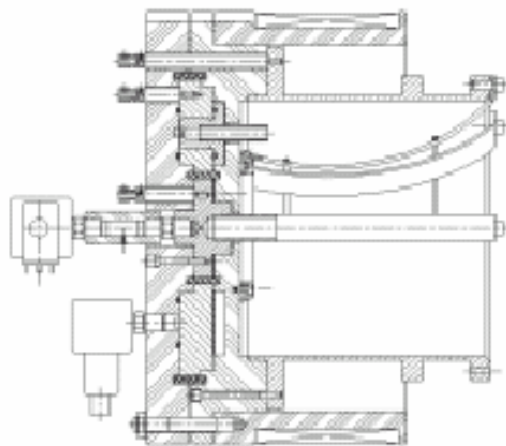


*Figure 2.1 – Schematic drawing of the MPD thruster assembly.*

It is an axisymmetric applied field Magneto-Plasma-Dynamic thruster (also said Hybrid Plasma Thruster, HPT). The thruster consists of a central copper hollow cathode (20 mm diameter, 50 mm length), through which 70-90% of gaseous propellant is injected in the discharge chamber, a cylindrical aluminium anode (200 mm inner diameter, 180 mm length) and eight copper straps which divide a central chamber from peripheral chamber. The remain part of propellant is injected through eight peripheral copper electrodes (12 mm diameter each). These electrodes can be used to

pre-ionize the peripheral propellant by means of a secondary discharge with the anode. These electrodes were not activated during all the tests described herein. A 70-turns coil surrounds the thruster and can be powered to generate a magnetic field up to 100 mT on the thruster axis (figure 2.2).



*Figure 2.2 – Picture of the MPD thruster.*

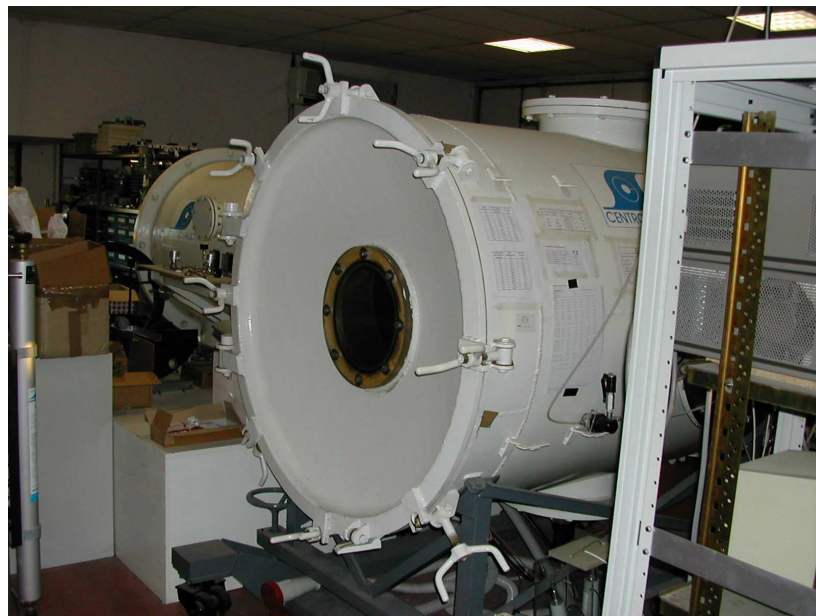


*Figure 2.3 – Picture of the IV3 vacuum chamber.*

The propellant is injected by two gas feeding systems, one for the central cathode and the other for peripheral cathodes, based on fast acting solenoid valves, which provide gas pulses with long plateau after few milliseconds from valve activation [20]. When a steady state mass flow is reached, the electric circuit is closed and the discharge takes place. A DC generator, switched on few seconds before the discharge, supplies the solenoid. The thruster is mounted on a thrust stand inside the Centropazio IV3 vacuum chamber shown in the figure 2.3, capable of maintaining a backpressure during the pulse in the  $10^{-4}$  mbar range.

A Pulse Forming Network (PFN), configured to supply quasi-steady current pulse 2.5 ms long, provides the electric power to the thruster. In figure 2.4, typical current and voltage signals are shown.

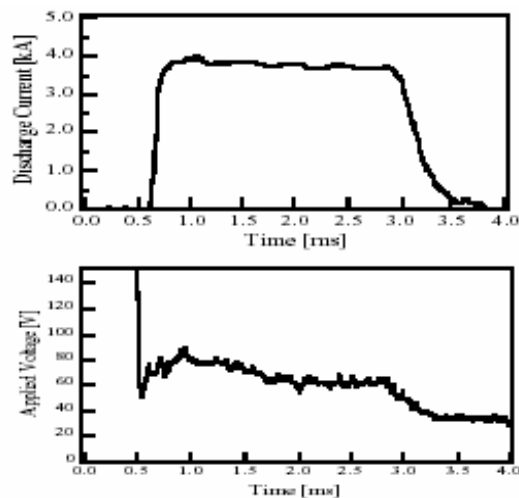


*Figure 2.4 – Discharge current and arc voltage vs. time.*

### 2.1.3 Thruster performance

Figures 2.5 and 2.6 show the electrical characteristics and the thrust of the thruster under investigation. For each discharge pulse, current and voltage were measured by averaging on 100 ms in the middle of the pulse.

The value of the thrust was obtained by a ballistic method by measuring the impulse of the thrust. Finally, the thrust is obtained by dividing the measured impulse by the pulse duration.

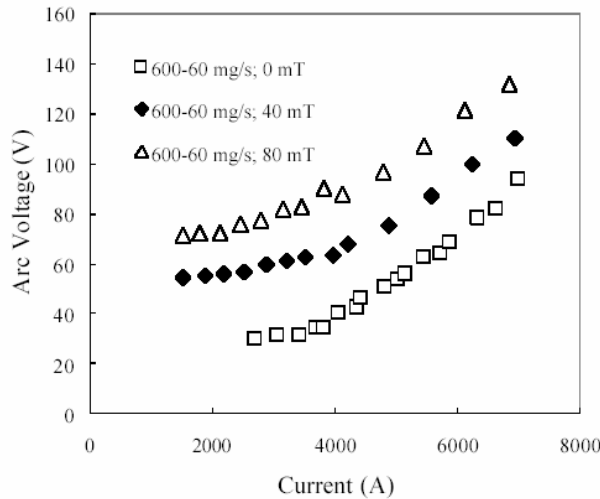


**Figure 2.5** – Electrical characteristic at 660 mg/s of argon.

Thus the value represents an average thrust during pulse time. Each point in figure 2.5 and figure 2.6 is obtained as an average of the values measured during four or five pulses at the same nominal conditions.

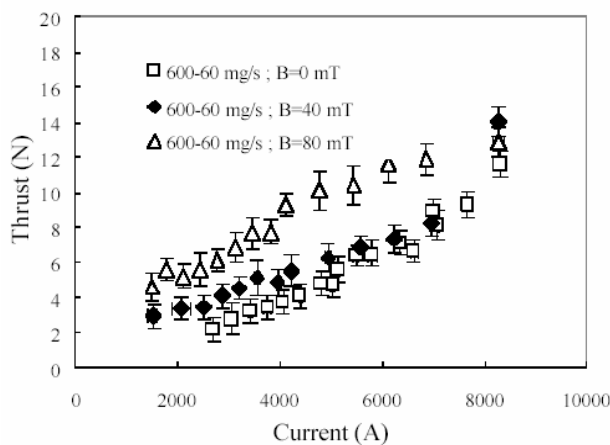


**Figure 2.6** – Thrust at 660 mg/s of argon.

Current and voltage measurements showed a good repeatability (the uncertainty is within the marker dimension). Error bars on thrust measurements include both the standard deviation and the measurement uncertainty (about 10% of the thrust value) [21], [23]. A clear increasing of arc voltage is observed when the external magnetic field is switched on (see figure 2.5).

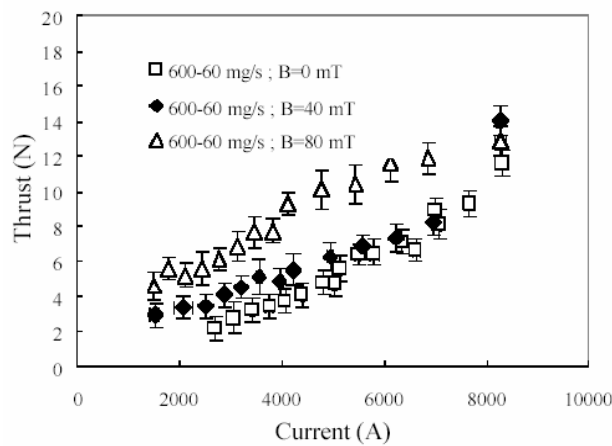


*Figure 2.6 – Thrust at 660 mg/s of argon.*

At the contrary the thrust (see figure 2.6) is almost the same in a self-field operation as with an applied field of 40 mT up to an arc power of about 500 kW and is lower in the latter case at higher power. Higher performance is obtained with an applied field of 80 mT. Nevertheless, the thrust reaches the same value of self-field operation at about 900 kW.

#### 2.1.4 Set-up of the spectroscopic measurements

The emitted radiation by the plasma is collected by an optical multi-channel analyzer (OMA) coupled to a CCD camera. The wavelength range simultaneously recorded by spectrograph is 200-1100 nm with a constant spectral resolution ( $\lambda/\Delta\lambda = 900$ , where  $\lambda$  is actual wavelength and  $\Delta\lambda$  the

wavelength resolution). A PCI-board permits the interactions between the CPU and the OMA system. The data acquisitions are controlled via software, by which is possible to configure both the time acquisition and the delay time from the TTL signal that activates the start of the measurement.

For a better knowledge of the plasma conditions in this MPD thruster, the emitted radiations are collected from different locations. So, the detector is placed both outside (non intrusive measurements) and inside (intrusive measurements) the vacuum chamber.

#### 2.1.4.1 Non intrusive collecting probe and test conditions

The OMA detector is a compact lens system that with focal length variable from 8 cm to 100 cm. The detector is placed out of the vacuum chamber at 70 cm from thruster axis. The image focus is 8 cm away from the thruster outlet (see figure 2.7).

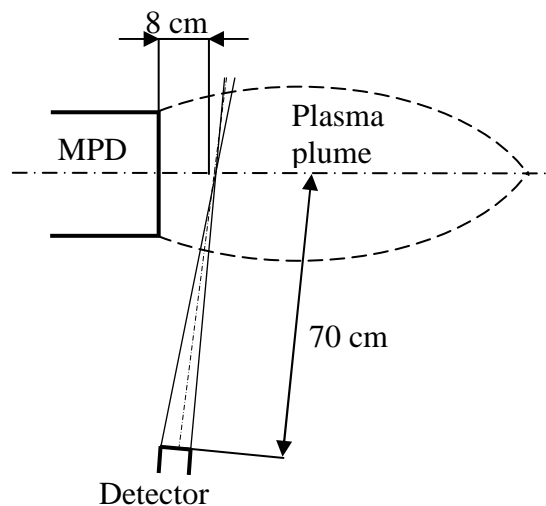


**Figure 2.7** - Schematic representation of the optical system with the detector placed outside the vacuum chamber.

This is the same position of electron temperature and density measurements performed on this thruster by other research group with Langmuir probes [29], [34]. The region of the plasma observed is a cylinder with a circular cross section of approximately 10 mm diameter.

Tests are performed using argon as propellant at a mass flow rate of 660 mg/s (600 mg/s injected through the central cathode and 60 mg/s through peripheral electrodes). The discharge current is varied from 4 kA to 8 kA both with and without the external applied magnetic field. Values of the magnetic field on the thruster axis are of 40 and 80 mT. The exposition times are fixed at 0.5 ms. In the table 2.1 below the detailed test conditions are reported. Each recorded spectrum is an average of three measurements at the same nominal conditions to reduce the background noise.

<u>Discharge current</u> I [A]	<u>External magnetic field</u> B [mT]	$\Delta t$ [ms]		
4500	0	0-0.5	0.5-1	1-1.5
6000	0	0-0.5	0.5-1	1-1.5
6500	0	0-0.5	0.5-1	1-1.5
7000	0	0-0.5	0.5-1	1-1.5
7500	0	0-0.5	0.5-1	1-1.5
4500	40	0-0.5	0.5-1	1-1.5
6500	40	0-0.5	0.5-1	1-1.5
7500	40	0-0.5	0.5-1	1-1.5
4500	80	0-0.5	0.5-1	1-1.5
6500	80	0-0.5	0.5-1	1-1.5
7500	80	0-0.5	0.5-1	1-1.5

*Table 2.1 – MPD test conditions with the non-intrusive probe.*

#### **2.1.4.2 Intrusive collecting probe and test conditions**

In order to collect the radiation from the ionization chamber of the MPD thruster, an optical probe containing the OMA detector inserted into

the plasma is utilized. The optical probe is realized by means of an optical fiber, coupled to a collimator of an achromatic doublet with a focal length of 30 mm. The whole system is encapsulated in Pyrex glass tube. As shown in figure 2.8, the probe is placed in six different positions. The optical axis of the probe in position 1, 2, 3, 4, 5 is parallel to the axis of the thruster. In position 6, it is perpendicular to the thruster axis.

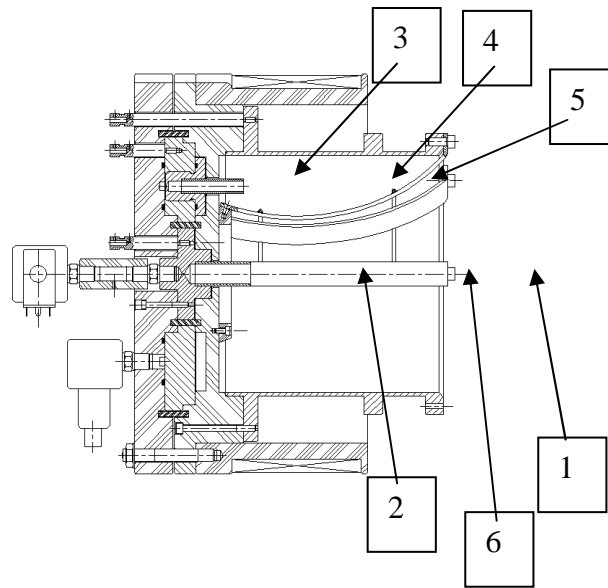


*Figure 2.8 - Overview of the various position of collecting spectra by means of the optical fiber probe.*

The detailed explanation of the probe disposition is the following:

1. Probe placed on the thruster axis at 80 mm from the thruster outlet with the focal point 50 mm away from it.
2. Probe placed on the thruster axis inside the ionization chamber at 10 mm from the thruster outlet with the focal point 40 mm away from it.
3. Probe placed in peripheral position inside the pre-ionization chamber with the focal point 50 mm away from the bottom of the chamber.
4. Probe placed in peripheral position inside the pre-ionization chamber with the focal point 140 mm away from the bottom of the chamber.

5. Probe placed in peripheral position between the anodic straps with the focal point 170 mm away from the bottom of the chamber.
6. Probe placed in perpendicular position at 0 mm from the thruster outlet with focal point on thruster axis.

In figures 2.9, 2.10 and 2.11, three pictures of the probe respectively in position 6 and 5 and 2 are shown.

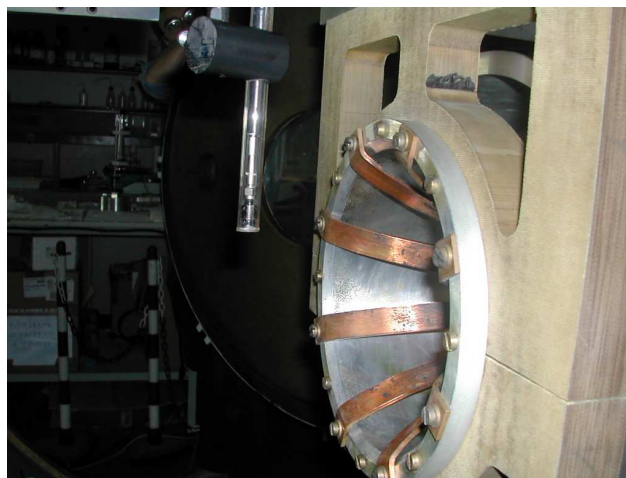


*Figure 2.9 - Picture of the probe inside the vacuum chamber referred as position 6 in the figure 2.8.*

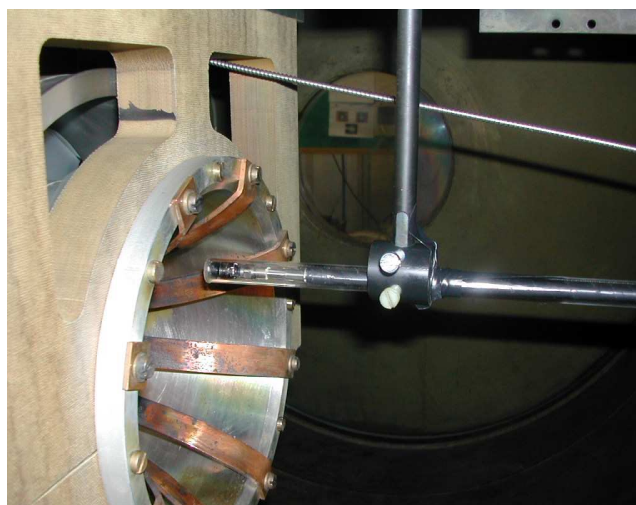


*Figure 2.10 - Picture of the probe inside the vacuum chamber referred as position 5 in the figure 2.8.*

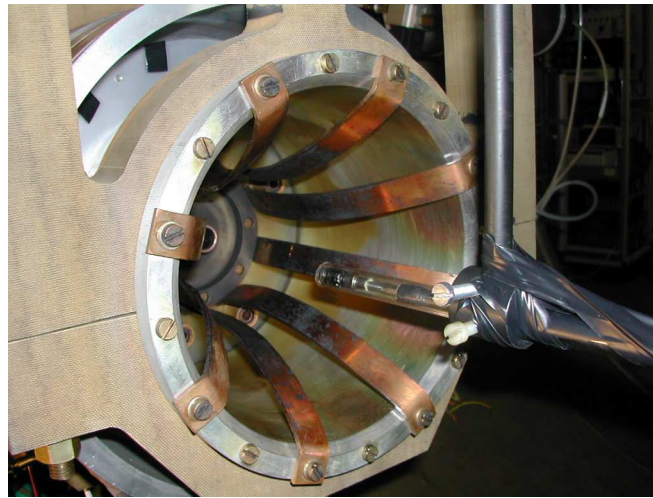


**Figure 2.11** - Picture of the probe inside the vacuum chamber referred as position 2 in the figure 2.8.

Also in this case, tests are performed using argon as propellant at a mass flow rate of 660 mg/s. The discharge current is varied from 4 kA to 8 kA both with and without the external applied magnetic field. Values of the magnetic field on the thruster axis are of 40 and 80 mT. The emitted radiation is recorded both during the start-up phase and the regime phase of the discharge current with different exposition times. In the table 2.2 below the detailed test conditions are reported.

<u>Discharge current</u> I [A]	<u>External magnetic field</u> B [mT]	<b>(1)</b>		<b>(2)</b>	<b>(3)</b>	<b>(4)</b>	<b>(5)</b>	<b>(6)</b>	
		$\Delta t$ [ms]							
4500	0	0-0.25	0.5-0.75	0.5-0.55	0.5-1	0.5-1	0.5-1	0-0.5	0.5-1
6000	0	0-0.25	0.5-0.75	0.5-0.55	0.5-1	0.5-1	0.5-1	0-0.5	0.5-1
7500	0	0-0.25	0.5-0.75	0.5-0.55	0.5-1	0.5-1	0.5-1	0-0.5	0.5-1
4500	80	0-0.25	0.5-0.75	0.5-0.55	0.5-1	0.5-1	0.5-1	0-0.5	0.5-1
6000	80	0-0.25	0.5-0.75	0.5-0.55	0.5-1	0.5-1	0.5-1	0-0.5	0.5-1
7500	80	0-0.25	0.5-0.75	0.5-0.55	0.5-1	0.5-1	0.5-1	0-0.5	0.5-1

**Table 2.2** – MPD test conditions with the intrusive probe. The numbers indicate the positions of the probe shown in figure 2.7.

For the probe in position 1 and 6, each recorded spectrum is an average of three measurements at the same nominal conditions in order to reduce the background noise.



*Figure 2.12 - Picture of the coat formed on the probe.*

In the other positions, the probe is highly sensitive to the impurities present in the plasma (mostly copper due to electrode erosion) which form a coat on it resulting in a progressive degradation of the probe transparency. So, the whole sequence has been completed (discharge current and external applied magnetic field) before to repeat the measurement other two times. This procedure also permits to evaluate qualitatively the impact of the coat on the recorded spectrum.

### **2.1.5 Imaging of the plasma plume: set-up and test conditions**

The imaging diagnostic is performed by means of a Pco Sensicam CCD color fast shutter camera. This CCD has got the useful capability to extend the exposing time till 100 ns. Its quantum efficiency has got a peak of approximately 40% at 500 nm: so, in this specific case, the light recorded comes predominantly from singly ions argon emission. It is also possible to

perform a double exposition, in order to evaluate the velocity of potential structures in the plasma plume. The imaging camera is positioned outside the vacuum chamber in correspondence of the its three optical windows. Two of them are perpendicular to the thruster axis. The other one is at 45° and enables the complete view of the ionization chamber. For all positions an F1 Canon 8-48 mm objective is used.

Only four conditions corresponding to the couples discharge current – impressed magnetic field reported in the table 2.3 are investigated. The image is recorded both during the start-up phase and the regime phase of the discharge current with different exposition times. The trigger event is fixed at the beginning of the rising edge of the current.

<u>Discharge current</u> I [A]	<u>External magnetic field</u> B [mT]
5000	0
7500	0
4500	80
7500	80

*Table 2.3 – MPD test conditions with the imaging camera.*

In order to point out the shape of the structures founded in the plasma plume, all the images are afterward elaborated at the computer with non-linear “stretching” techniques.

## **2.2 The RF discharge reactor**

### **2.2.1 Theory of dust particle formations**

Nowadays, two mechanisms of dust formation in silane plasmas are generally accepted. The first model considers a four-step mechanism using

charged particles clusters [51]-[57]. In the first phase primary clusters are formed, as a result of molecular and ion polymerisation chemistry (see figure 2.13a). Negative ions play an important role in the polymerization at low pressures due to their good electric confinement and because of high rates of ion-induced reactions. Under the right condition, the primary clusters nucleate and grow into nanometer sized structures (figure 2.13b). Once these nanometer sized particles, with fluctuating but small positive or negative charges, reach a critical density of  $10^{15}$ – $10^{18}$   $\text{m}^{-3}$ , a rapid agglomeration takes place (figure 2.13c). At the end of this phase, the plasma contains permanently negatively charged clusters with a diameter of 20-50 nm at a density of  $10^{12}$ – $10^{15}$   $\text{m}^{-3}$ .

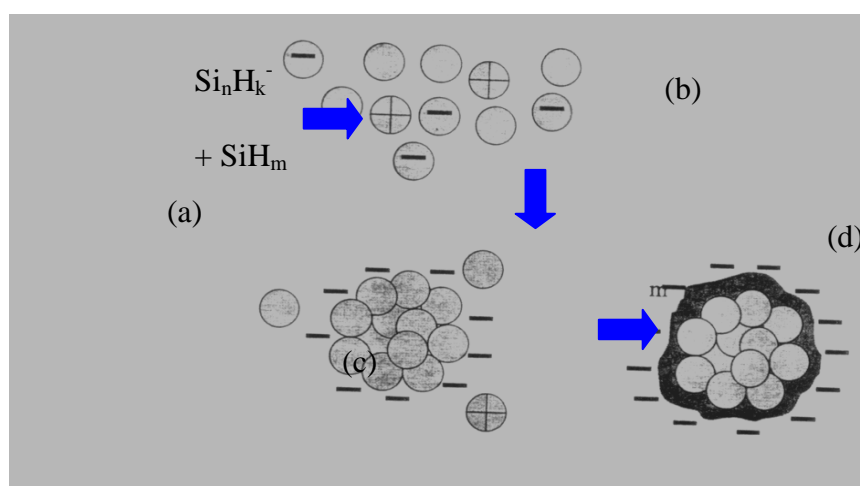


**Figure 2.13** – Schematic view of the “four-step” formation mechanism of particles in silane plasmas: (a) primary clusters, (b) nucleation, (c) agglomeration phase and formation of larger cluster and (d) growth due to deposition of plasma species.

The charging of the particles is also evidenced from the depletion of the electron density. After the coagulation phase, the particles grow steadily by deposition of plasma species (figure 2.13d). A second particle formation model favours neutral growth only by plasma polymerisation starting from  $\text{SiH}_x$  radicals [58]. Many authors have pointed out that the gas temperature is a critical parameter for a particle formation and their growth [59]-[60].

At increased temperatures, nano-particle nucleation is delayed in time and at sufficiently high temperatures (above 200 °C) particle formation does not proceed beyond nano-particles. These results are initially obtained by means of a detection method for small particles based on laser induced particle explosive evaporation (LIPEE) [58] and are recently confirmed using novel electrical measurements of plasma voltage and current [59].

### **2.2.2 Description of the experimental apparatus**

The radio-frequency (RF) discharge reactor, developed in the laboratories of the Department of Physics at the Eindhoven University of Technology (TU/e), is schematically described in the figure 2.13. The vacuum vessel is a grounded cylindrical stainless steel box of 300 mm external diameter and 500 mm height. The plasma is confined in an internal aluminium chamber of 140 mm internal diameter. The distance between the electrodes is 40 mm. The upper electrode is powered capacitively by an RF power supply at 13.56 MHz. The sidewalls and the bottom are grounded. Two thermocouples PT-100 and four heating elements located symmetrically around the upper electrode allow variations of gas and electrode temperature from room temperature to 180 °C. The 5% SiH<sub>4</sub> in Ar gas mixture flows vertically through the showerhead upper electrode and the bottom grid serving as grounded electrode. A mass-flow controller monitors the gas flow. The pressure is measured outside the discharge chamber by a Baratron capacitive gauge. Three slits in the inner cylindrical chamber and three windows on the vacuum chamber allow optical observations of the central region of the plasma. Observation slits and windows are aligned and placed at 90° from one another. In order to avoid spreading of the discharge outside the discharge chamber a mesh grid

covers each slit. The pumping system consists of a pre vacuum pump and a turbo-molecular pump achieving a base pressure below  $10^{-6}$  mbar.

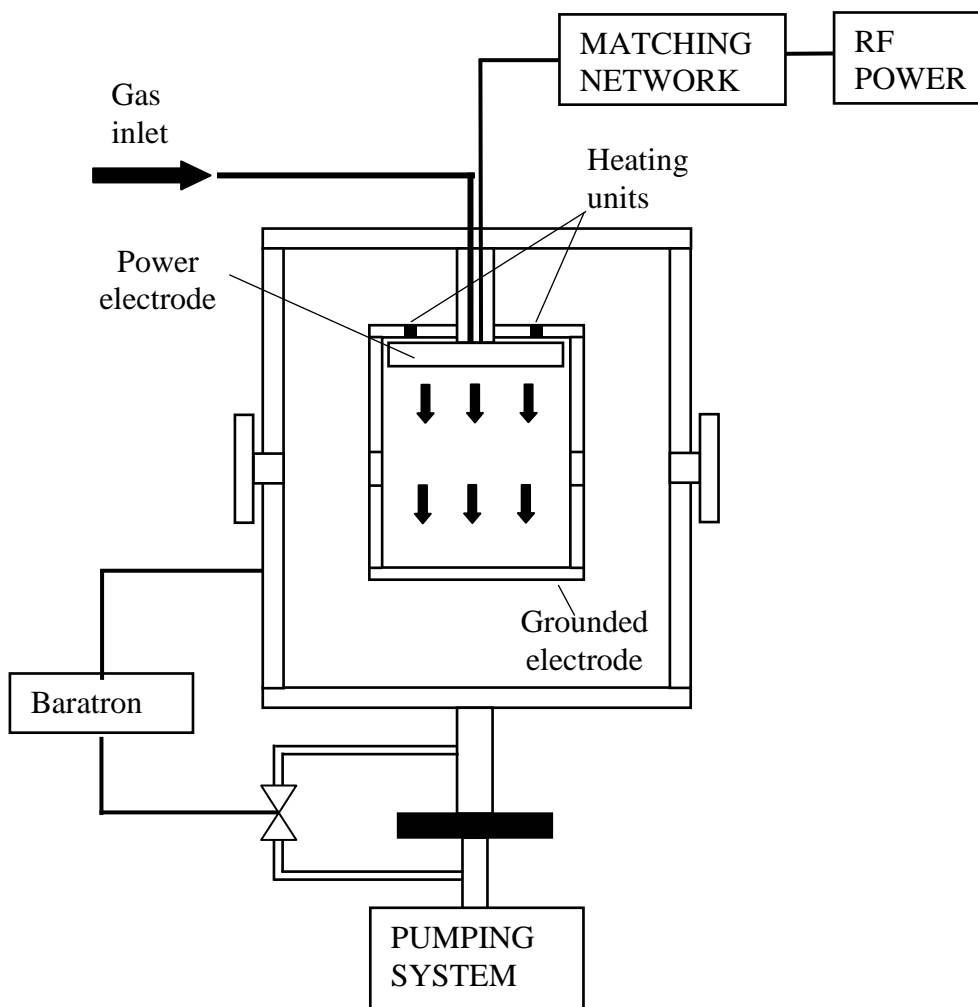


*Figure 2.14 – Scheme of the experimental RF discharge apparatus.*

### 2.2.3 Set-up of the optical measurements

An overview of the experimental set-up is shown in figure 2.15. The space integrated emission spectrum in the wavelength range of 400 - 900 nm of the whole plasma region is analysed with the aid of an optical multichannel analyser: EG&G OMA III with a model 1420 intensified detector. An optical system of two spherical lenses  $L_1$  and  $L_2$  of focal

distance of 200 mm and 80 mm respectively focuses plasma light on a 2 mm optical fibre.

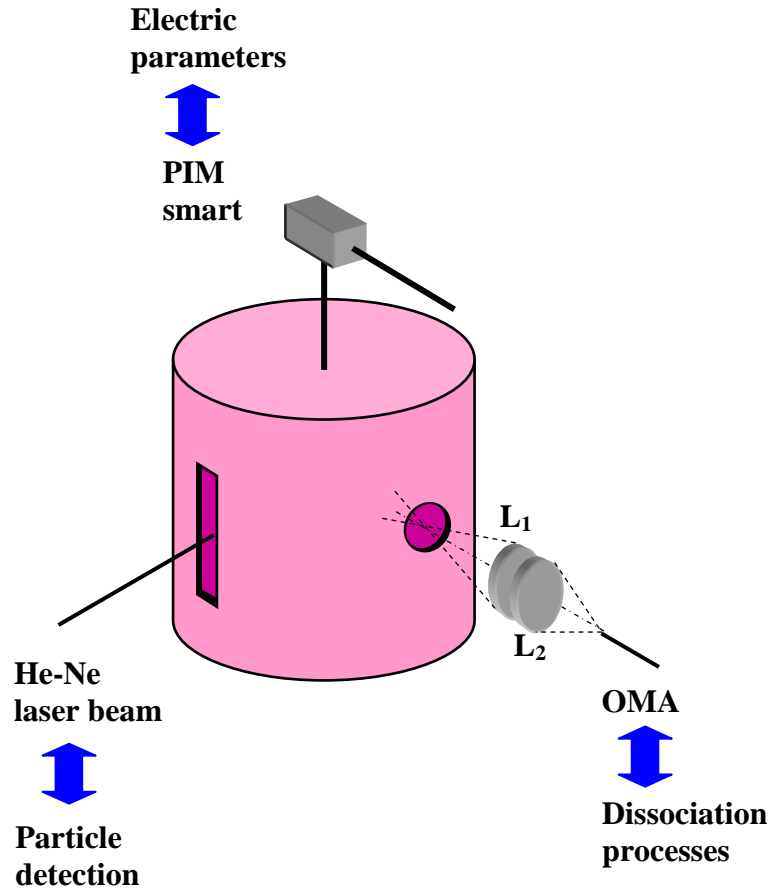


*Figure 2.15 – Overview of the electrical and optical diagnostics.*

The time behaviour of the first emission line of Hydrogen Balmer series  $H_{\alpha}$  at 656.2 nm and Si-H ( $A^2\Delta \rightarrow X^2\Pi$ ) band head at 414.2 nm are followed. These lines are taken as representatives of silane dissociation phenomena in the plasma. Laser-light scattering by a helium neon laser is used to detect particles bigger than about 20 nm in the centre of the discharge. The He-Ne laser beam (5 mW) is directed across the reactor through the two opposing light holes of 2 mm in diameter, which were made in the grid-slits. The scattered light is collected simultaneously with the plasma emission, perpendicular to the laser beam by the same optical

system described previously. In addition to the OMA system a video camera is used to monitor particles coming through the sidewall slits out of the discharge chamber.

### 2.2.4 Measurements of the electrical parameters

A commercial plasma impedance monitor the “Smart PIM” by Scientific Systems, allows the measurement of the RF current, voltage and phase angle in a real time regime. The voltage-current sensor is placed in the RF power line, between the RF reactor and the  $\Pi$ -type matching network, about 20 cm from the upper electrode (figure 2.15 and figure 2.16b).

The standard approach to sensing the current and voltage delivered to the process chamber is shown schematically in figure 2.16a. The RF current is measured by a single loop current sensor and the RF voltage by a capacitive pickup placed near the RF power conductor. The voltage sensor is capacitively coupled to the RF power conductor and is terminated by a  $50\ \Omega$  resistance. The current sensor is inductively coupled to the RF power conductor and is also terminated by a  $50\ \Omega$  resistance.

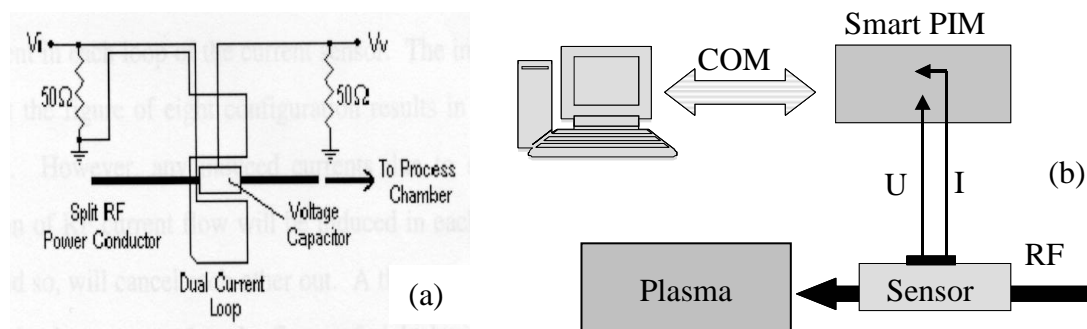


**Figure 2.16** – Scheme of the voltage-current sensor(a) and layout of the electrical measurements (b).

To reduce the effects of stray voltage pickup, a grounded shield protects the loop of the current sensor. This shield acts as a Faraday shield and reduces the amount of voltage pickup that the loops detect.

The system also calculates the RF power and the plasma impedance and provides information about the harmonic content of all electrical parameters up to the fifth harmonic. A full view of the experimental set-up is shown in the figure 2.17, in which the identification of the PIM sensor and the He-Ne laser is reported.

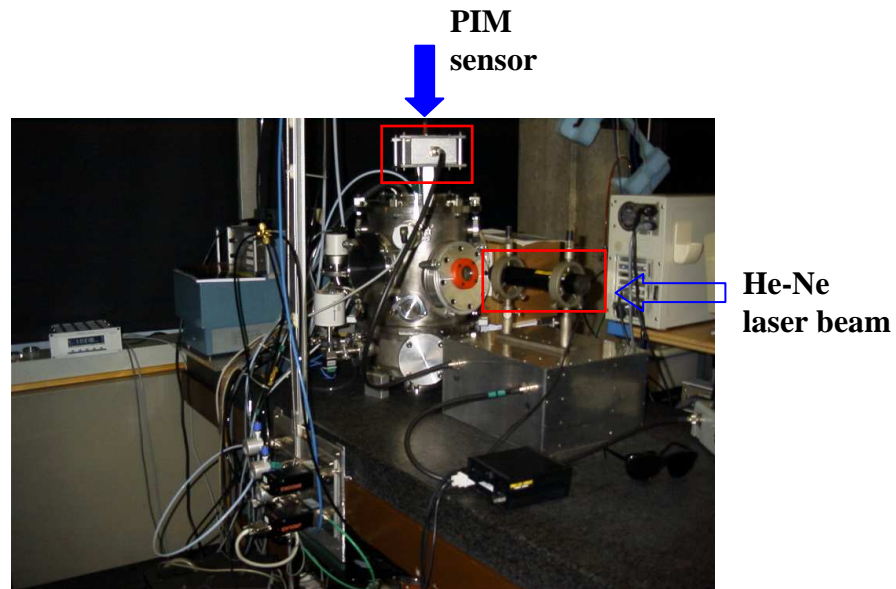


*Figure 2.17 - Picture of the RF reactor experimental set-up.*

### 2.2.4 Test conditions

The experiments reported here are performed in an argon-silane mixture containing 5% of silane, at a pressure of 0.133 mbar (100 mTorr) and a gas flow rate of 10 sccm. The forward RF power is 10 W, which corresponds to power density of  $1.6 \times 10^{-2} \text{ mW/mm}^3$ .

All measurements are carried out with a constant value of the reflected power corresponding at approximately 30% of the direct power. For all the

measurements, the exposition time of the OMA system is fixed at  $\Delta t = 1$  s. Between two consecutive exposition, an interval time of approximately 1 second is taken.